Journal of Materials Chemistry A

PAPER

View Article Online
View Journal | View Issue

CrossMark click for updates

Cite this: J. Mater. Chem. A, 2014, 2, 14164

Immobilization of a *N*-substituted azaphosphatrane in nanopores of SBA-15 silica for the production of cyclic carbonates†

Bastien Chatelet,[a] Lionel Joucla,[a] Jean-Pierre Dutasta,[a] Alexandre Martinez*[a] and Véronique Dufaud*[b]

Received 28th March 2014
Accepted 25th June 2014

DOI: 10.1039/c4ta01500b

www.rsc.org/MaterialsA

A novel *N*-substituted azaphosphatrane molecular precursor bearing an alkyne tether was synthesized using a multi-step strategy and covalently immobilized onto SBA-15 type silica through triazole linkages by means of the well-known click chemistry. The resulting hybrid material, **[7]@SBA-15**, was characterized well by methods appropriate to molecular species (*e.g.* solid state ^{13}C, ^{31}P and ^{29}Si NMR, infrared spectroscopy and elemental analysis) as well as techniques more commonly associated with the characterization of mesoporous solids (nitrogen sorption isotherms, powder X-ray diffraction, TGA analysis). The catalytic activity of **[7]@SBA-15** was then evaluated in the coupling of CO_2 with two epoxides (styrene oxide and epichlorohydrin) and compared to its monotriazole modified AZAP molecular analog, **8**. This work represents the first example of silica modified *N*-substituted azaphosphatrane for the production of cyclic carbonates.

1. Introduction

Proazaphosphatranes Verkade's superbases have recently attracted considerable interest as highly active and selective basic or nucleophilic catalysts in a wide range of organic transformations.[1–9] These cyclic aminophosphines, built from the tris(2-aminoethyl)-amine (tren) scaffold, exhibit strong basicity ($pK_a \sim 32$) owing to their ability to become protonated on their phosphorus atom rather than on the nitrogen atoms, unlike all the commonly used non-ionic bases. As a result, the tricyclic conjugated acids thus obtained, called azaphosphatranes (AZAP), are remarkably stable. It is perhaps because they are so stable that few synthetic or catalytic studies involving these molecules have been undertaken as opposed to the widely studied conjugated base proazaphosphatranes. For instance, one can cite their use as procatalysts in combination with sodium hydride for the conversion of bromoalkanes to alkenes[10] or their ability to promote Michael and Strecker reactions.[11] We have recently demonstrated that these azaphosphatrane salts could also act as versatile phase transfer catalysts in a number of alkylation, oxidation and cyclopropanation organic reactions[12] and more interestingly that they could efficiently promote the coupling of carbon dioxide, a renewable feedstock, with epoxide to produce cyclic carbonates under atmospheric pressure.[13] Although homogeneous catalysts are ideal for fine-tuning reactivity and selectivity of a specific transformation, their separation from the reaction mixture and subsequent purification are energy-consuming and often troublesome, generating a large amount of wastes. Heterogeneous catalysts, on the other hand, provide easier separation, recovery and reusability of the catalyst and are more suited for use in industrial processes and continuous-flow operations. One promising approach to combine the advantages associated with both types of catalysts is the direct immobilization of relevant homogeneous catalytic species onto insoluble supports whether organic or inorganic. Several methodologies are currently available for this purpose including entrapment, adsorption, ion-pair formation and covalent binding, thus leading to a wide variety of hybrid catalytic materials.[14–18] Surprisingly, examples of solid-supported azaphosphatranes are rare. To the best of our knowledge, there are only two papers dealing with the immobilization of azaphosphatranes onto polymeric supports. In those reports, the covalent link to the surface was achieved by reacting one of the equatorial amino groups with a chloromethylated Merrifield's peptide resin under fairly drastic conditions (DMF, 110 °C, 6 days). The resulting solid catalyst was successfully applied in various organic transformations (dehydrohalogenation,[10] Michael and Strecker reactions[11]) and was found to be highly recyclable.

[a]*Laboratoire de Chimie, École Normale Supérieure de Lyon, CNRS, UCBL, 46 allée d'Italie, 69364 Lyon, France. E-mail: Alexander.Martinez@ens-lyon.fr; Fax: +33 4727 28860; Tel: +33 4727 28863*

[b]*Laboratoire de Chimie, Catalyse, Polymère, Procédés (C2P2), CNRS, Université Claude Bernard Lyon1, CPE Lyon, 43 Bd du 11 novembre 1918, 69616 Villeurbanne Cedex, France. E-mail: Veronique.Dufaud@univ-lyon1.fr; Fax: +33 4724 31795; Tel: +33 4724 31792*

† Electronic supplementary information (ESI) available: Synthesis of molecular model **8**, NMR data of compounds **7** and **8**. For **[7]@SBA-15** and parent **[N_3]@SBA-15** hybrids: physical properties, solid-state ^{29}Si NMR, TGA, elemental analyses and FT-IR. TEM/EDX for **[7]@SBA-15**. See DOI: 10.1039/c4ta01500b

Although interesting, this approach is exclusively limited to non-substituted azaphosphatranes. We have recently shown that the substitution pattern on the AZAP catalyst greatly affects its activity and stability in the synthesis of cyclic carbonates.[13] Thus, diversifying the electronic and steric properties of azaphosphatranes, notably by changing auxiliary groups on the equatorial nitrogen atoms, is highly desirable to test for structure–activity relationships and optimize the catalyst properties.

In our approach to provide a graftable anchor while keeping the substitution versatility, we chose to desymmetrize the substituents on the equatorial amines of the tren unit. As we shall see, the synthesis of such molecular precursors involves a multistep protection/deprotection strategy using appropriately functionalized aldehydes. Further immobilization onto SBA-15 type silica was achieved through covalent bonding using the well-known click chemistry since this reaction proceeds with high yields under mild conditions.[19] Beyond recycling and separation advantages, the immobilization of AZAP in the inner space of mesoporous SBA-15 silica may provide beneficial changes in reactivity owing to its high specific surface area (up to 1000 $m^2\ g^{-1}$) and tunable ordered pore systems (2–100 nm). The state of the solid structure and the integrity of the immobilized azaphosphatrane were characterized by several methods including X-ray powder diffraction at small angles, elemental analysis, thermogravimetric analysis, infrared spectroscopy, multi-nuclei solid state NMR spectroscopy, nitrogen sorptions and transmission electron microscopy (TEM). Finally, the catalytic performance of the resulting organic–inorganic hybrid material was examined in the cycloaddition of CO_2 to epoxides and compared to its soluble clicked analogue. To the best of our knowledge, this work represents the first example of silica modified *N*-substituted azaphosphatrane for the production of cyclic carbonates.

2. Experimental

2.1 General

All manipulations were conducted under a strict inert atmosphere or vacuum conditions using Schlenk techniques including the transfer of the catalysts to the reaction vessel. The solvents were dried using standard methods and stored over activated 4 Å molecular sieves. Tetraethoxysilane (TEOS) and poly(ethyleneoxide)–poly(propyleneoxide)–poly(ethyleneoxide) block copolymer (Pluronic 123, M_w 5000) were purchased from Aldrich Chemicals. CO_2 of a purity of 99.99% was commercially obtained and used without further purification. (3-Chloropropyl)triethoxysilane was purchased from ABCR. (3-Iodopropyl)triethoxysilane was prepared by reacting (3-chloropropyl) triethoxysilane with NaI in refluxing acetone for 72 hours according to the method described by Matsura *et al.*[20] (3-Azidopropyl)triethoxysilane was synthesized by reacting 3-iodopropyltriethoxysilane with an excess of sodium azide (5 eq.) in dry DMF at 50 °C for 72 hours by adapting a procedure described elsewhere.[21] Azidobutane was prepared by reacting 1-bromobutane and sodium azide in dry DMF at 60 °C for 24 hours. Compound **1** was synthesized by following a procedure described in the literature.[22] *p*-Propargyloxybenzaldehyde was synthesized from *p*-hydroxybenzaldehyde and 3-bromo-1-propyne according to a procedure described in the literature.[23]

2.2 Synthesis of molecular compounds

Synthesis of compound 2. *p*-Anisaldehyde (9.6 mL, 78.9 mmol) was added to a solution of protected tren **1** (8.00 g, 32.5 mmol) in 250 mL of methanol. The reaction mixture was stirred overnight. $NaBH_4$ (5.96 g, 157.8 mmol) was then added to the ice-cooled solution. The mixture was allowed to warm up to room temperature and the solvent was evaporated. 10% aqueous NaOH (250 mL) was then added and the mixture was extracted with dichloromethane (3 × 200 mL). The combined organic phases were dried over Na_2SO_4, filtered and the solvent was removed under vacuum. The crude compound was purified by column chromatography on silica gel using a (90 : 10 : 2) mixture of dichloromethane, methanol and triethylamine as an eluent to give compound **2** as a yellow oil (12.18 g, 77%). ν_{max} cm^{-1} 3305 (br), 2962, 2933, 2832, 1707 s (C=O), 1513 s, 1247, 1174 (C–N), 813. δ_H (500.1 MHz; $CDCl_3$) 7.22 (4H, d, J_3 8.77, ArH), 6.84 (4H, d, J_3 8.77, ArH), 3.78 (6H, s, OCH_3), 3.70 (4H, s, NCH_2Ar), 2.66–2.63 (5H, m, NCH_2CH_2N), 2.60–2.57 (5H, m, NCH_2CH_2N), 2.55–2.53 (2H, m, NCH_2CH_2N), 1.43 (9H, m, NBoc). δ_C (125.7 MHz; $CDCl_3$) 158.7 (C=O), 156.3 (C_{Ar}), 131.9 (C_{Ar}), 129.5 ($C_{Ar}H$), 113.9 ($C_{Ar}H$), 78.9 ($C(CH_3)_3$), 55.3 (OCH_3), 54.1 (NCH_2Ar), 54.0 (NCH_2CH_2N), 53.1 (NCH_2CH_2N), 46.8 (NCH_2CH_2N), 39.07 (NCH_2CH_2N), 28.5 ($(-CH_3)_3$). ESI-MS *m*/*z* obsd 487.3271 $[M + H]^+$, calcd 486.3206 for $C_{27}H_{42}N_4O_4$.

Synthesis of compound 3. To an ice-cooled solution of compound **2** (12.18 g, 25.03 mmol) in 80 mL of dry THF was added triethylamine (9.8 mL, 72.58 mmol). *o*-Nitrobenzenesulfonylchloride (12.59 g, 56.82 mmol) was then added portion-wise to the mixture. The reaction mixture was allowed to warm up to room temperature and stirred overnight. The solvent was removed under vacuum and the residue was dissolved with 10% aqueous K_2CO_3 (250 mL) prior to be extracted with dichloromethane (3 × 250 mL). The combined organic phases were dried over Na_2SO_4, filtered and the solvent was removed under vacuum. The crude compound was purified by column chromatography on silica gel using a 98 : 2 mixture of dichloromethane and methanol as the eluent to give compound **3** as a yellow oil (17.34 g, 77%). ν_{max} cm^{-1} 3419 (br), 2975, 2935, 2836, 1706 s (C=O), 1544 (C_{Ar}–NO_2), 1513, 1367 (C_{Ar}–NO_2), 1249, 1160 (S=O), 1033 (C–N), 779. δ_H (500.1 MHz; $CDCl_3$) 7.95 (2H, d, J_3 7.60), 7.70–7.63 (6H, m, ArH), 7.14 (4H, d, J_3 8.59, ArH), 6.81 (4H, d, J_3 8.59, ArH), 4.36 (4H, s, NCH_2Ar), 3.77 (6H, s, OCH_3), 3.17 (4H, t, J_3 7.50, NCH_2CH_2N), 2.90–2.89 (2H, m, NCH_2CH_2N), 2.30–2.27 (6H, m, NCH_2CH_2N), 1.43 (9H, m, NBoc). δ_C (125.7 MHz; $CDCl_3$) 159.5 (C=O), 156.0 (C_{Ar}), 148.0 (C_{Ar}), 133.5 ($C_{Ar}H$), 133.4 (C_{Ar}), 131.9 ($C_{Ar}H$). 130.9 ($C_{Ar}H$), 129.9 ($C_{Ar}H$), 127.4 (C_{Ar}), 124.2 ($C_{Ar}H$), 114.2 ($C_{Ar}H$), 79.0 ($C(CH_3)_3$), 55.3 (OCH_3), 53.9 (NCH_2Ar), 52.3 (NCH_2CH_2N), 51.8 (NCH_2CH_2N), 45.5 (NCH_2CH_2N), 38.3 (NCH_2CH_2N), 28.4 ($-C(CH_3)_3$). ESI-MS *m*/*z* obsd 857.2809 $[M + H]^+$, calcd 857.2844 for $C_{39}H_{49}N_6O_{12}S_2$.

Synthesis of compound 4. To an ice-cooled solution of compound **3** (17.24 g, 20.12 mmol) in 135 mL of dichloromethane was added 135 mL of trifluoroacetic acid. The reaction

mixture was stirred for one hour at 0 °C and then allowed to warm up to room temperature. The solvents were evaporated. Aqueous 10% NaOH was added and the mixture was extracted with dichloromethane (3 × 250 mL). The combined organic phases were dried over Na_2SO_4, filtered and the solvent was removed under vacuum to give **4** as a yellow oil (14.71 g, 97%). ν_{max} cm^{-1} 3348 (br), 2935, 2836, 1542 (C_{Ar}–NO_2), 1511, 1346 (C_{Ar}–NO_2), 1160 (S=O), 1031 (C–N). δ_H (500.1 MHz; $CDCl_3$) 7.98 (2H, d, J_3 7.60), 7.67–7.60 (6H, m, ArH), 7.14 (4H, d, J_3 8.73, ArH), 6.80 (4H, d, J_3 8.73, ArH), 4.35 (4H, s, NCH_2Ar), 3.76 (6H, s, OCH_3), 3.25 (3H, t, J_3 7.22, NCH_2CH_2N), 2.66 (2H, t, J_3 5.50, NCH_2CH_2N), 2.45–2.43 (3H, m, NCH_2CH_2N), 2.29 (4H, t, J_3 7.22, NCH_2CH_2N). δ_C (125.7 MHz; $CDCl_3$) 159.5 (C_{Ar}), 147.9 (C_{Ar}), 133.6 ($C_{Ar}H$), 133.1 (C_{Ar}), 132.1 ($C_{Ar}H$), 130.9 ($C_{Ar}H$), 130.0 ($C_{Ar}H$), 127.4 (C_{Ar}), 124.2 ($C_{Ar}H$), 114.2 ($C_{Ar}H$), 55.3 (OCH_3), 54.0 (NCH_2Ar), 52.4 (NCH_2CH_2N), 51.7 (NCH_2CH_2N), 45.8 (NCH_2CH_2N), 38.5 (NCH_2CH_2N). ESI-MS *m*/*z* obsd 757.2315 $[M + H]^+$, calcd 757.2320 for $C_{34}H_{41}N_6O_{10}S_2$.

Synthesis of compound 5. *p*-Propargyloxybenzaldehyde (3.708 g, 23.15 mmol) was added to a solution of compound **4** (14.60 g, 19.29 mmol) in 80 mL of methanol. The reaction mixture was stirred overnight. $NaBH_4$ (1.751 g, 46.30 mmol) was then added to the ice-cooled solution. The mixture was then allowed to warm up to room temperature and the solvent was evaporated. 10% aqueous NaOH (250 mL) was added and the mixture was extracted with dichloromethane (3 × 200 mL). The combined organic phases were dried over Na_2SO_4, filtered and the solvent was removed under vacuum. The crude compound was purified by column chromatography on silica gel using a 96 : 4 mixture of dichloromethane and methanol as the eluent to give compound **5** as a yellow oil (16.19 g, 93%). ν_{max} cm^{-1} 3390 (br), 3286 (≡C–H), 2933, 2836, 2119 w (C≡C), 1542 s (C_{Ar}–NO_2), 1346 (C_{Ar}–NO_2), 1247, 1160 (S=O), 1027 (C–N). δ_H (500.1 MHz; $CDCl_3$) 7.95–7.93 (2H, m, ArH), 7.70–7.61 (6H, m, ArH), 7.30 (2H, d, J_3 8.54, ArH), 7.10 (4H, d, J_3 8.73, ArH), 6.91 (2H, d, J_3 8.65, ArH), 6.78 Hz (4H, d, J_3 8.73), 4.66 (2H, d, J_3 2.35), 4.33 (4H, s, NCH_2Ar), 3.75 (8H, s, OCH_3 and NCH_2Ar), 3.17 (4H, t, J_3 7.30, NCH_2CH_2N), 2.51 (1H, t, J_3 2.35, C≡C–*H*), 2.48 (4H, t, J_3 2.35, NCH_2CH_2N), 2.29 (4H, t, J_3 7.30, NCH_2CH_2N). δ_C (125.7 MHz; $CDCl_3$) 159.5 (C_{Ar}), 157.2 (C_{Ar}), 148.0 (C_{Ar}), 133.3 (C_{Ar}), 133.6 ($C_{Ar}H$), 133.2 (C_{Ar}), 132.0 ($C_{Ar}H$), 130.9 ($C_{Ar}H$), 130.0 ($C_{Ar}H$), 128.6 ($C_{Ar}H$), 127.4 (C_{Ar}), 124.3 ($C_{Ar}H$), 115.0 ($C_{Ar}H$), 114.2 ($C_{Ar}H$), 78.6 (*C*≡C–H), 75.7 (C≡*C*–H), 55.9 (O*C*H_2C≡H), 55.3 (OCH_3),53.5 (NCH_2Ar), 52.6 (NCH_2N), 52.3 (NCH_2CH_2N), 51.7 (NCH_2CH_2N), 46.1 (NCH_2CH_2N), 45.7 (NCH_2CH_2N). ESI-MS *m*/*z* obsd 901.2873 $[M + H]^+$, calcd 901.2895 for $C_{44}H_{49}N_6O_{11}S_2$.

Synthesis of compound 6. To a solution of compound **5** (16.09 g, 17.86 mmol) in 300 mL of DMF was added Na_2CO_3 (18.08 g, 170.5 mmol). Thiophenol (10.1 mL, 98.68 mmol) was added under vigorous stirring. The reaction mixture was heated to 50 °C for 24 hours. The solvent was evaporated and water (300 mL) was added to the residue and the mixture was extracted with dichloromethane (3 × 300 mL). The solvent was evaporated up to 200 mL and the organic phase was extracted with 1 N aqueous HCl. NaOH pellets were added to the combined aqueous phases until pH 12 was reached. The solution was extracted with dichloromethane (3 × 200 mL). The combined organic phases were dried over Na_2SO_4, filtered and the solvent was removed under vacuum to give **6** (5.433 g, 57%) as a yellow oil. ν_{max} cm^{-1} 3390 (br), 3288 (≡C–H), 2958, 2931, 2832, 2111 w (C≡C), 1610, 1511 s, 1454, 1245, 1031 (C–N). δ_H (500.1 MHz; $CDCl_3$) 7.19–7.15 (6H, m, ArH), 6.87 (2H, d, J_3 8.58, ArH), 7.81 (4H, d, J_3 8.65, ArH), 4.62 (2H, d, J_4 2.35, OCH_2C≡C), 3.77 (6H, s, OCH_3), 3.66 (6H, s, NCH_2Ar), 2.66 (6H, t, J_3 5.50, NCH_2CH_2N), 2.58 (6H, m, NCH_2CH_2N), 2.49 (1H, t, J_3 2.35, C≡C–*H*). δ_C (125.7 MHz; $CDCl_3$) 158.7 (C_{Ar}), 156.7 (C_{Ar}), 132.9 (C_{Ar}), 131.8 (C_{Ar}), 129.5 ($C_{Ar}H$), 129.5 ($C_{Ar}H$), 114.8 ($C_{Ar}H$), 113.8 ($C_{Ar}H$), 78.6 (*C*≡C–H), 75.6 (C≡*C*–H), 55.8 (O*C*H_2C≡H), 55.3 (OCH_3), 54.1 (NCH_2Ar), 54.0 (NCH_2Ar), 53.1 (NCH_2CH_2N), 46.9 (NCH_2CH_2N), 46.8 (NCH_2CH_2N). ESI-MS *m*/*z* obsd 531.3318 $[M + H]^+$, calcd 531.3330 for $C_{32}H_{43}N_4O_3$.

Synthesis of propargyl azaphosphatrane 7. In an ice-bath cooled round bottomed flask, tris(dimethylamino)phosphine (1.340 mL, 7.37 mmol) was dissolved in acetonitrile (70 mL). Phosphorus trichloride (0.322 mL, 3.69 mmol) was then added drop-wise. The reaction mixture was vigorously stirred at 0 °C for 0.5 h, and a solution of **6** (5.33 g, 10.05 mmol) in acetonitrile (35 mL) was introduced drop-wise. The reaction mixture was then stirred for 2 days at room temperature. The solvent was removed under reduced pressure and the resulting yellow oil was purified by column chromatography on silica gel using a 15 : 1 mixture of dichloromethane and methanol as the eluent to give compound **7** as an orange oil (3.41 g, 60%). ν_{max} cm^{-1} 3390 (br), 3291 (≡C–H), 2111 w (C≡C), 1610, 1511, 1245, 1120, 1034, 740. δ_H (500.1 MHz; $CDCl_3$) 7.08 (2H, d, J_3 8.64, ArH), 7.06 (4H, d, J_3 8.60, ArH), 6.94 (2H, d, J_3 8.64, ArH), 6.85 (4H, d, J_3 8.68), 5.79 (1H, d, $^1J_{P\text{-}H}$ 497), 4.68 (2H, d, J_4 2.38, OCH_2C≡C), 4.11 (2H, d, $^3J_{P\text{-}H}$ 16.90, $ArCH_2N$), 4.06 (4H, d, $^3J_{P\text{-}H}$ 17.10, $ArCH_2N$), 3.80 (6H, s, OCH_3), 3.60–3.58 (6H, m, NCH_2CH_2N), 3.07–3.03 (6H, m, NCH_2CH_2N), 2.53 (1H, *t*, J_4 2.35, C≡C–H). δ_C (125.7 MHz; $CDCl_3$) 159.4 (C_{Ar}), 157.3 (C_{Ar}), 130.2 (C_{Ar}), 129.1 (C_{Ar}), 128.8 ($C_{Ar}H$), 128.8 ($C_{Ar}H$), 115.5 ($C_{Ar}H$), 114.5 ($C_{Ar}H$), 78.4 (*C*≡C–H), 75.9 (C≡*C*–H), 56.0 (O*C*H_2C≡H), 55.5 (O*C*H_3), 50.9 (N*C*H_2Ar, d, J_3 16.1), 50.8 (N*C*H_2Ar, d, J_3 16.1), 47.1 (NCH_2CH_2N, d, J_3 7.3), 39.3 (NCH_2CH_2N, m). δ_P (202.4 MHz; $CDCl_3$) −12.16 (d, $^1J_{P\text{-}H}$ 497). ESI-MS *m*/*z* obsd 559.2829 $[M]^+$, calcd 559.2833 for $C_{32}H_{40}N_4O_3P^+$.

Synthesis of clicked model 8 (Scheme S1† in ESI). To a solution of compound **7** (274 mg, 0.460 mmol) in 6 mL of dichloromethane was added diisopropylethylamine (0.5 mL, 2.76 mmol), 92 mg of azidobutane (0.92 mmol) and a catalytic quantity of CuI. The reaction mixture was stirred overnight. The organic phase was washed with a diluted aqueous ammonia solution, twice with water, dried over Na_2SO_4, filtered and the solvent was removed under vacuum. The crude compound was purified by column chromatography on silica gel using a 10 : 1 mixture of dichloromethane and methanol as the eluent to give compound **8** as a brown oil (220 mg, 69%). ν_{max} cm^{-1} 2930, 2862, 1609, 1509, 1240, 1169, 1102, 1029. δ_H (500.1 MHz; $CDCl_3$) 7.65 (s, triazole), 7.11–7.08 (6H, m, ArH), 6.98 (2H, d, J_3 8.52, ArH), 6.87 (4H, d, J_3 8.56, ArH), 5.79 (1H, d, $J_{P\text{-}H}$ 497), 5.21 (2H, s, OCH_2, triazole), 4.37 (2H, t, J_3 7.33, triazoleCH_2), 4.13 (6H, d, $^3J_{P\text{-}H}$ 16.92, $ArCH_2N$), 3.81 (6H, s, OCH_3), 3.52 (6H, m, NCH_2CH_2N), 3.10 (6H, m, NCH_2CH_2N), 1.90 (2H, q, J_3 7.43, triazoleCH_2CH_2), 1.37 (2H, sex, J_3 7.45, triazole$CH_2CH_2CH_2$),

0.96 (3H, t, J_3 7.45, triazole$CH_2CH_2CH_2CH_3$). δ_C (125.7 MHz; $CDCl_3$) 159.4 (C_{Ar}), 158.2 (C_{Ar}), 143.9 (C_{Ar}), 129.9 ($C_{triazole}$=$C_{triazole}$H), 129.2 (C_{Ar}), 129.0 (C_{Ar}H), 123.0 ($C_{triazole}$=$C_{triazole}$H), 115.5 (C_{Ar}H), 114.6 (C_{Ar}H), 62.3 (OCH_2, triazole), 55.6 (OCH_3), 51.1 (NCH_2Ar), 50.4 (triazoleCH_2), 47.9 (NCH_2CH_2N), 39.5 (NCH_2CH_2N), 32.4 (triazoleCH_2CH_2), 19.9 (triazole$CH_2CH_2CH_2$), 13.6 (triazole$CH_2CH_2CH_2CH_3$). δ_P (202.4 MHz; $CDCl_3$) −11.19 (d, $^1J_{P\text{-}H}$ 497). ESI-MS *m*/*z* obsd 658.3602 $[M]^+$, calcd 658.3629 for $C_{36}H_{49}N_7O_3P$.

2.3 Hybrid silica materials

One-pot synthesis of azide functionalized SBA-15 silica, [N_3]@SBA-15. SBA-15 mesoporous silica containing azidopropyl groups was prepared by a one-pot co-condensation procedure. In a typical experiment, P123 (5.06 g, 0.87 mmol) was weighed into a Teflon bottle. Then 2.0 M HCl (150 mL, 300 mmol) and H_2O (7.5 mL, 416.66 mmol) were added and the mixture was stirred at 40 °C until the P123 was fully dissolved. TEOS (9.6 g, 46.08 mmol) was then added to the reaction and stirred at 40 °C for 1 hour prehydrolysis time. (3-Azidopropyl)triethoxysilane (0.20 g, 0.60 mmol) was introduced dropwise into the reaction mixture which was subsequently stirred at 40 °C for 20 hours, aged at 100 °C for 24 hours, and then cooled to room temperature. The resulting solid was filtered and repeatedly rinsed with H_2O and Et_2O. The solid was then allowed to dry overnight on an aspirating filter. The dried solid was Soxhlet extracted with MeOH for 24 hours to remove P123. The white solid was finally dried overnight at 60 °C under vacuum and stored under nitrogen, **[N_3]@SBA-15**.

Click reaction of azaphophatrane 7 onto [N_3]@SBA-15. [N_3]@SBA-15 (3 g) was suspended in dry THF (70 mL) followed by subsequent addition of azaphosphatrane **7** (590 mg, 0.850 mmol), diisopropylethylamine (10 equivalents) and a catalytic quantity of CuI (0.2 equivalent). The reaction was stirred for 2 days at room temperature. After filtration, the solid was washed thoroughly with THF. The resulting solid was then contacted with 0.1 M of *N*,*N*-diethyldithiocarbamate sodium in MeOH (15 mL) to remove CuI and further washed with methanol (20 mL), THF (10 mL) and acetone (10 mL). The final hybrid material denoted **[7]@SBA-15** was dried overnight at 60 °C under vacuum and stored under nitrogen.

2.4 Characterization

Small-angle X-ray powder diffraction (XRD) data were acquired on a Bruker D5005 diffractometer using Cu Kα monochromatic radiation (λ = 1.5418 Å). Nitrogen adsorption–desorption isotherms at 77 K were measured using a Micromeritics ASAP 2020M physisorption analyzer. The samples were evacuated at 120 °C for 24 h before the measurements. Specific surface areas were calculated following the BET procedure. Pore size distribution was obtained by using the BJH pore analysis applied to the desorption branch of the nitrogen adsorption–desorption isotherm. A Netzsch thermoanalyser STA 409 PC was used for simultaneous thermal analysis combining thermogravimetric (TGA) and differential thermoanalysis (DTA) at a heating rate of 10 °C min^{-1} in air from 25–900 °C. Solid state CP-MAS experiments were performed on a Bruker DSX 500 spectrometer using a 4 mm double resonance Bruker MAS probe at spectral frequencies of 99.3 and 125.7 MHz for respectively ^{29}Si and ^{13}C nuclei. Chemical shifts were referenced to TMS. The spinning rate was 10 or 15 kHz and samples were spun at the magic angle using ZrO_2 rotors. The experimental details for the ^{29}Si and ^{13}C CP-MAS NMR experiments were as follows: contact time: 5 ms and 2 ms respectively, number of scans: 3000 to 25 000 and repetition time: 2 s. ^{31}P MAS NMR spectra were recorded on a Bruker DSX-500 spectrometer operating at 202.4 MHz with a classical 4 mm probehead allowing spinning rates up to 10 kHz. The spectra were obtained by direct irradiation of phosphorus and proton decoupling. In all cases it was checked that there was a sufficient delay between the scans (5000) allowing a full relaxation of the nuclei. The chemical shifts are given relative to external 85% H_3PO_4. Liquid NMR spectra of molecular compounds were recorded on a Bruker AC-500 spectrometer and referenced as following: ^1H (500.1 MHz) and ^{13}C (125.7 MHz) chemical shifts were measured relative to residual ^1H or ^{13}C resonances in $CDCl_3$: δ 7.26 ppm for ^1H, 77 ppm for ^{13}C and ^{31}P (202.4 MHz) referenced to external 85% H_3PO_4 at δ = 0.00 ppm. Data are reported as follows: chemical shift, number of equivalent nuclei, multiplicity (s = singlet, d = doublet, t = triplet, q = quartet, sex = sextuplet, m = multiplet), coupling constant (*J* in Hz), and assignment. During catalytic runs, yields were estimated by ^1H NMR with a Bruker Avance 300 spectrometer at 300.1 MHz. Mass spectral analyses were performed on a Nermag R10-10C for exact mass. Elemental analyses were obtained from the University of Bourgogne and the Research Institute on Catalysis and Environment of Lyon. C, N, P elemental analyses determinations were performed by ICP-AES (Activa Jobin Yvon) spectroscopy from a solution obtained by treatment of the solid catalyst with a mixture of HF, HNO_3 and H_2SO_4 in a Teflon reactor at 150 °C. Fourier transform infrared spectra (FT-IR) were recorded using a JASCO FT/IR-4200 (JASCO) spectrometer in the transmittance mode. Transmission electron microscopy (TEM) was performed with a 200 kV JEOL 2100F microscope, with a point to point resolution of 0.23 nm. This instrument was equipped with an EDS X-ray analyzer LINK-ISIS. The preparation of the sample was performed by dispersing the catalyst powder on a microscopy copper grid (3.05 mm; 200 mesh) previously coated with a holey-carbon film.

2.5 Catalytic testing

[7]@SBA-15 (597 mg containing 0.05 mmol of azaphosphatrane) or compound **8** (34.7 mg, 0.05 mmol), epichlorohydrin or styrene oxide (5 mmol), 2,4-dibromomesitylene (used as internal standard) and toluene (1 mL) were loaded into a 30 mL stainless autoclave. The reactor was flushed three times at room temperature with 10 bar of CO_2 to remove air from the vessel before being further charged to 20 bar of CO_2 and raised to 80 °C. After the desired reaction time (24 hours), the reactor was cooled to room temperature and then in an ice bath and finally the excess of CO_2 was carefully released. In the case of **[7]@SBA-15**, the solid was washed with chloroform and the mixture was centrifuged. The procedure was repeated three times and the

supernatant was collected. Reaction yields were determined by ^{1}H NMR after removal of the solvent.

3. Results and discussion

3.1 Synthesis of the AZAP precursor containing a clickable anchor

Among the different methods reported in the literature for anchoring organic molecules onto oxide surfaces, we have identified the copper(I)-catalyzed azide–alkyne 1,3-dipolar cycloaddition as a highly efficient and reliable ligation process to create robust linkages.[19] The first step to attain this purpose was the synthesis of a *N*-substituted AZAP molecular precursor bearing an alkyne tether. This was achieved using a multi-step strategy which allowed for the selective introduction of various substituents at the nitrogen atoms of the tren unit, as depicted in Scheme 1. The synthesis starts from commercially available tren, whose one of the amine functions was selectively monoprotected with a Boc group, **1**.[22] The two remaining free amines were then reacted with *p*-methoxybenzaldehyde *via* a reductive alkylation to afford **2** in 77% yield. In order to prevent reaction of the two newly formed secondary amines with *p*-propargyloxybenzaldehyde, these latter were subsequently protected with *o*-nitrobenzenesulfonylchloride to yield *N,N*-disubstituted-2-nitrobenzenesulfonamide **3**. The *N*-Boc protected group could then be selectively removed with trifluoroacetic acid and the resulting free amine cleanly reacted with *p*-propargyloxybenzaldehyde to give the *N*-alkylated product **5**. Upon treatment with PhSH and Na_2CO_3 in DMF at 50 °C, facile deprotection of **5** *via* a S_NAr reaction mechanism[24] was carried out leading to the formation of functionalized tren ligand **6**. Finally, the phosphorus could be inserted following the classical procedure described by Verkade[25] to give the dissymmetric propargyl azaphosphatrane **7** in 60% yield. Structural characterization of compounds **1–7** was assessed using FT-IR, multinuclei NMR spectroscopy and electrospray ionisation mass spectrometry (ESI-MS) (Experimental section). In the particular case of **7**, ^{31}P NMR confirmed the successful incorporation of the phosphorus atom in the tren ligand as the ^{31}P NMR spectrum exhibits a single resonance at −12.2 ppm typical of the PH site for AZAP derivatives (ESI, Fig. S3†).

3.2 Synthesis of the AZAP organic–inorganic hybrid material

In the design of hybrid materials, the influence of host matrix parameters such as pore size and morphological topology can be effectively controlled and adapted to the guest size. In this regard, SBA-15 silica,[26] which possesses a regular hexagonal 2D structure, represents an attractive host for the immobilization of catalytically relevant species. Because of its high surface area and high silanol density, SBA-15 is easy to functionalize, and its large pore diameter allows for large molecules to enter the pores with less mass transfer limitation than materials with a smaller pore size (*i.e.* MCM-41 silica). In this study, we used a two-step procedure to prepare clean azaphosphatrane functional silica surfaces (Scheme 2). SBA-15 mesoporous silica modified by azidopropyl groups was first synthesized by the one-pot co-condensation route since this approach provides for greater homogeneous distribution of functional groups within the solid.[27] After removal of the P123 structure directing agent, **[N$_3$]@SBA-15** was reacted with azaphosphatrane **7** under classical

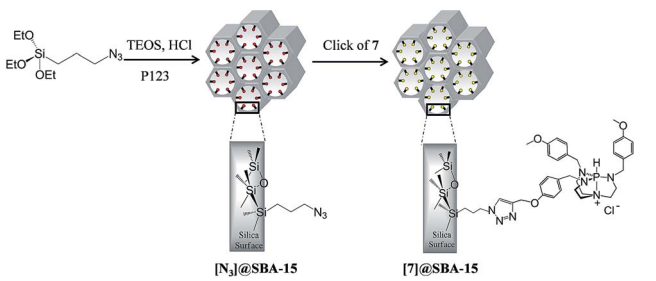

Scheme 2 Immobilization of azaphosphatrane through click chemistry.

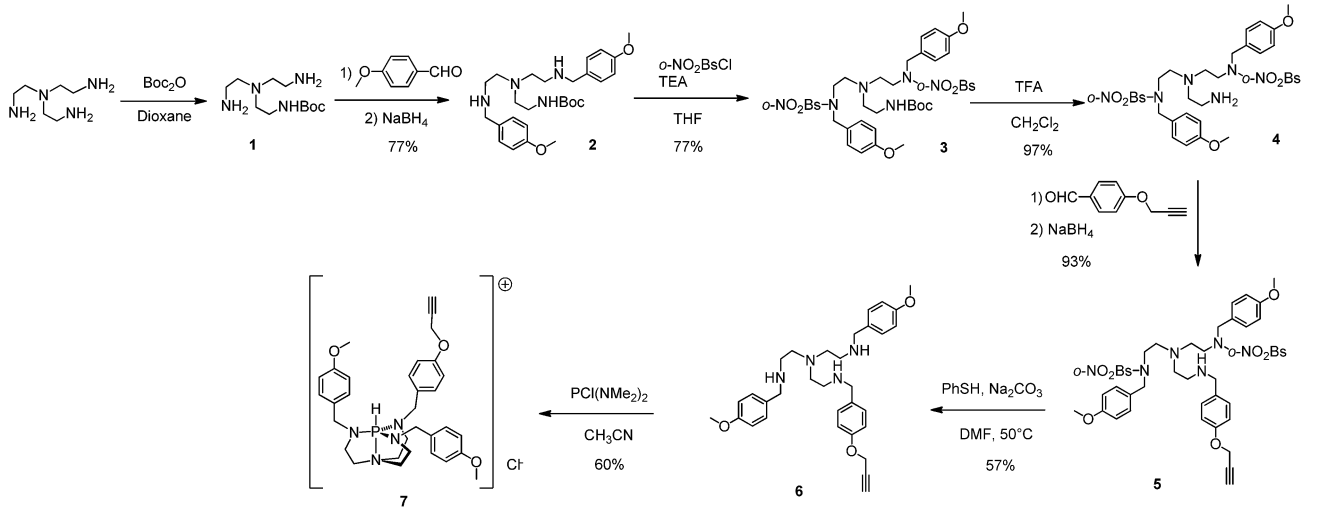

Scheme 1 Synthesis strategy to alkyne-containing azaphosphatrane.

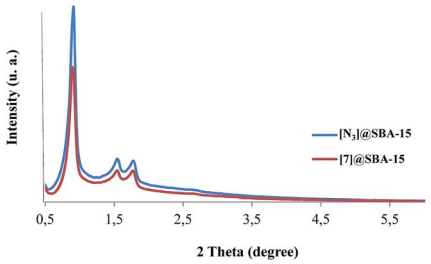

Fig. 1 X-ray powder diffraction patterns of the azide functionalized SBA-15 silica material before and after click reaction of **7**.

click conditions in the presence of diisopropylethylamine and a catalytic amount of CuI, yielding hybrid **[7]@SBA-15**.

The physicochemical and textural properties of hybrid materials derived from powder XRD and sorption measurements are summarized in Table S1† (ESI). Small angle powder XRD patterns of SBA-15 materials collected before and after click reaction of **7** are displayed in Fig. 1. Both solids exhibited typical diffractograms characteristic of hexagonally ordered mesophases with the presence of three well resolved peaks in the 2θ-range of 0.6 to 2° attributed respectively to (100), (110) and (200) reflexions. The presence of higher order reflexions indicates that the chemical bonding procedure did not diminish the long-range structural ordering in the materials although a slight decrease in intensity of the d100 reflection was observed for **[7]@SBA-15**. The ordering was also clearly evident in the TEM/EDX imagery with a homogeneous distribution of azaphosphatrane **7** throughout the solid (ESI, Fig. S7 and Table S2†).

Nitrogen adsorption–desorption measurements were used to examine the textural properties of the hybrid materials. Typical isotherms and pore size distributions are depicted in Fig. 2. Both materials showed type IV isotherms and H1 hysteresis loop characteristic of mesoporous solids and SBA architectures. A steep capillary condensation step appearing at $P/P_0 = 0.6$–0.8 (Fig. 2, top) indicated the presence of regular mesopores in the samples which was further confirmed by a narrow pore size distribution in the mesopore range (Fig. 2, bottom). Upon derivatization of **[N$_3$]@SBA-15** with azaphosphatrane **7**, no change in pore diameter was observed (~58 Å) whereas a marked decrease in the BET surface area (from 594 $m^2\ g^{-1}$ to 415 $m^2\ g^{-1}$, Table S1†) and pore volume (from 0.89 $cm^3\ g^{-1}$ to 0.65 $cm^3\ g^{-1}$, Table S1†) was noted which is consistent with the presence of a significant amount of azaphosphatrane on the interior mesopore surfaces.

The successful incorporation of **7** in **[N$_3$]@SBA-15** was further confirmed by solid-state ^{13}C and ^{31}P NMR spectroscopy. Examination of the ^{13}C NMR spectrum of **[7]@SBA-15** showed the presence of two key peaks at 122 and 145 ppm typical of the triazole ring suggesting that **7** has been efficiently attached to the azide linker without measurable degradation as most resonances of the azaphosphatrane fragment were also discernible (Fig. 3).

Further information concerning the phosphorus environment in **[7]@SBA-15** was obtained from CP MAS ^{31}P NMR. As shown in Fig. 4, a single broad resonance centered at −12.8 ppm along with spinning side bands was observed. The absence of significant shift when compared to the liquid ^{31}P spectrum of **7** suggests that the AZAP moiety remained intact upon click reaction. The P–H site seems unaffected by inclusion of the AZAP moiety in the silica matrix probably due to the protection provided by the lipophilic pocket formed by a ring of substituted benzyl-amino groups around the central PH unit.

The ^{29}Si CP MAS spectrum of **[7]@SBA-15** showed no significant changes compared to the parent **[N$_3$]@SBA-15** (ESI,

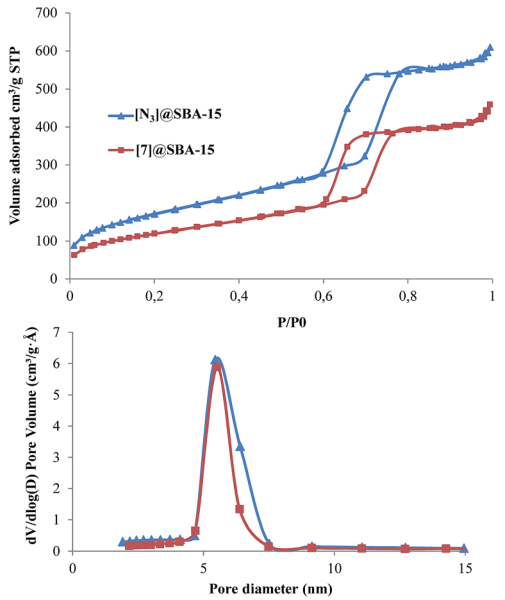

Fig. 2 Nitrogen adsorption–desorption isotherms (top) and pore size distributions (bottom) of azide **[N$_3$]@SBA-15** and clicked silica materials **[7]@SBA-15**.

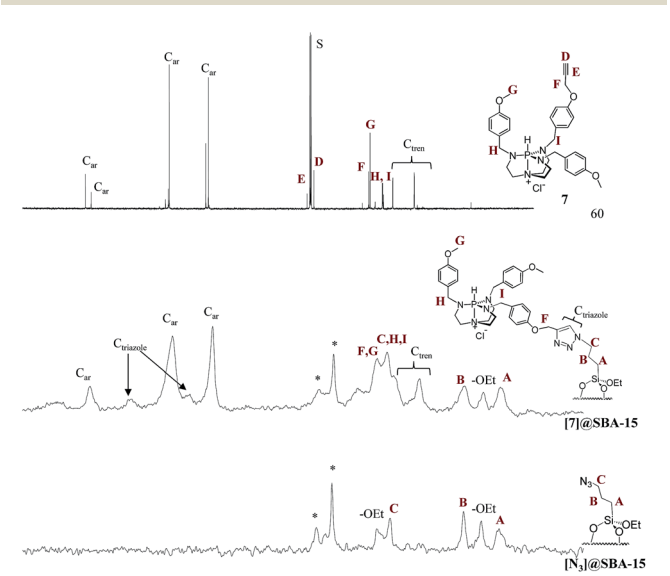

Fig. 3 CP MAS ^{13}C NMR of **[N$_3$]@SBA-15** before and after click reaction of **7** and the liquid ^{13}C NMR spectrum of molecular azaphosphatrane, **7** for comparison. S and * denote respectively $CDCl_3$ and P123.

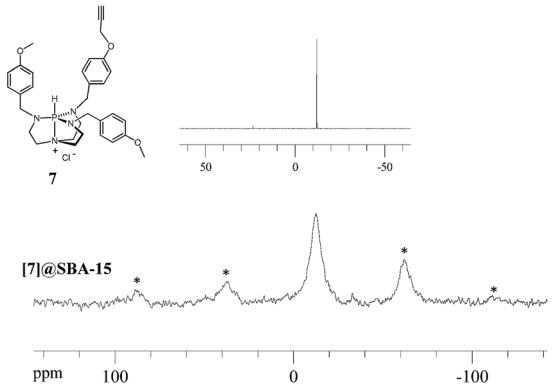

Fig. 4 Liquid ^{31}P NMR spectrum of molecular azaphosphatrane **7** and MAS ^{31}P NMR of **[7]@SBA-15**. * denotes spinning side bands.

Fig. S8†), indicating that the Si sites did not undergo any chemical changes during the course of the click reaction. Specifically, the peaks associated with organosiloxanes (T-type silicates) in the spectral region ranging from −60 to −75 ppm remained unchanged which is a clear indication that covalent bonding in **[N_3]@SBA-15** was unaffected by subsequent surface derivatization.

Quantitative determination of organic content was obtained from nitrogen and phosphorus elemental analyses. Thus, the functional group loading corrected from sample humidity, that is by considering the SiO_2 content of the TGA run at 1000 °C, was found to be 0.17 and 0.10 mmol g^{-1} dry silica for respectively **[N_3]@SBA-15** and **[7]@SBA-15** (Table S3†, ESI). This suggests that 60% of the surface azido groups in **[N_3]@SBA-15** were successfully attached to **7** through the triazole ring. This result was further confirmed by FT-IR, in particular by the decrease in intensity upon click reaction of the stretching vibration mode at 2117 cm^{-1} typical of organic azide (Fig. S9†, ESI). Thermogravimetric analysis before and after click reaction of **7** was also performed under flowing air from room temperature to 1000 °C (ESI, Fig. S10†). In general, similar thermal patterns, composed of three weight loss regions, were observed for both hybrids: the weight loss due to desorption of physisorbed water occurring before 170 °C was followed by a progressive weight loss comprised between 170 and 700 °C which was ascribed to organic species decomposition. Because of the presence of the remaining P123 structure directing agent in both solids, as evidenced by ^{13}C NMR, this weight loss could not be taken as a reliable estimate of the total amount of organics. The third weight loss region which took place above 700 °C was attributed to the release of water formed from the condensation of silanols in the silica matrix. Examination of the DTA curve of **[7]@SBA-15** reveals the presence of an additional sharp decomposition peak around 255 °C which could likely arise from the AZAP moiety desorption.

3.3 Coupling of CO_2 and epoxides to cyclic carbonates

As previously mentioned, the reactivity of the resulting organic–inorganic hybrid material **[7]@SBA-15** was then examined in the coupling of CO_2 with epoxides to produce cyclic carbonates. This atom-efficient industrial process which utilizes CO_2 as a raw material to value-added products has lately attracted considerable interest (Scheme 3).[28] Organic carbonates are important building blocks that have been widely applied as polar aprotic solvents, electrolytes for lithium batteries, monomers for polycarbonates and copolymers synthesis and as useful intermediates in the fine chemical and pharmaceutical industries.[29] Metal-free catalytic processes have existed for over 50 years, based mainly on quaternary ammonium or phosphonium salts,[30] but they require fairly drastic reaction conditions (high temperatures and pressures) and the use of relatively pure CO_2. Other viable processes based on more reactive transition metal catalysts[31] are productive under milder conditions, but in this case metal contamination of final products as well as catalyst separation and disposal becomes both an environmental and economic drawback. Therefore, the development of new technologies and metal-free catalysts that operate under mild reaction conditions is a priority to minimize costs and greenhouse gas emissions and provide true viable alternatives for fossil fuel-based chemicals.

In this regard, we have recently described the use of azaphosphatranes as original and tunable catalysts for the synthesis of cyclic carbonates from CO_2 and epoxides, hence demonstrating their utility as single components, metal-free alternatives to current state-of-the-art catalysts.[13] In particular, we have shown that the substitution around the reactive P–H site could have an impact on catalyst activity and stability. Thus, a molecular analog of the triazole linked supported catalyst was also synthesized to allow for meaningful comparative catalytic studies. It was obtained by reacting *n*-butylazide with AZAP **7** to afford a dissymmetric monotriazole modified AZAP **8**, in which the SBA-15 surface of **[7]@SBA-15** has been replaced by a methyl group (Scheme S1†, ESI).

In this paper, the comparison of the triazole-linked AZAP hybrid catalyst to the molecular analog was accomplished under identical conditions of temperature, CO_2 pressure, substrate concentration and, notably substrate/AZAP molar ratio using two epoxide substrates: styrene oxide and epichlorohydrin. Typical reaction conditions were as follows: 80 or 100 °C, 24 h, catalyst loading of 1 mol%, and 20 bar CO_2. Lower pressures (1 and 10 bar) were attempted but yields of product were insufficient for our purpose. Table 1 shows the test results. One can see that the molecular catalyst **8** leads to near-quantitative conversion of both phenyl-substituted and chloromethylene-substituted epoxides to the corresponding cyclic carbonates under these reaction conditions. The supported catalyst **[7]@SBA-15** was reactive and revealed that there was a substrate structural effect, the conversion of styrene oxide being limited to 21% whereas with epichlorohydrin a conversion of

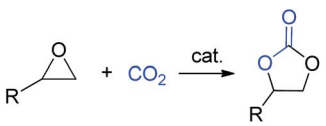

Scheme 3 Synthesis of cyclic carbonates from epoxides and carbon dioxide.

Table 1 Coupling of CO_2 and epoxides to cyclic carbonates[a]

Substrate	Temperature (°C)	Catalyst	Yield (%)
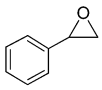	100	[7]@SBA-15	21
		8	99
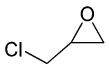	80	[7]@SBA-15	49
		8	99

[a] Conditions: epoxide (5.0 mmol), catalyst (0.05 mmol), toluene (1 mL), CO_2 (20 bar), and 24 hours. Yields were determined by ^{1}H NMR using 2,4-dibromomesitylene (1.0 mmol) as an internal standard.

49% could be achieved even at lower reaction temperature (80 °C). The decrease in activity of the AZAP catalyst when supported over SBA-15 support could stem from diffusion constraints due to the steric requirements of the bulky AZAP moiety within the pores of the material. The importance of free-space availability around the active site was stressed by Udayakumar *et al.* for ionic liquid-based MCM-41 catalytic systems as a key parameter for improved reactivity.[32]

Nevertheless, this work highlights that the catalytic properties of AZAP for the conversion of CO_2 and epoxides to cyclic carbonates were not inhibited by their heterogenization, paving the way towards the design of new hybrid materials with improved properties.

4. Conclusion

In this report, we have extended our studies of azaphosphatranes to include a heterogeneous version for use in the synthesis of cyclic carbonates. Thus, a *N*-substituted AZAP having a pendant alkyne group was synthesized and grafted to SBA-15 mesoporous silica using the easily generalizable click chemistry. The resulting material, in which an asymmetrically substituted AZAP ring was linked to the surface by a single organo-triazole unit, was finely characterized as both a bulk material and at the molecular level. The supported AZAP material was found to be catalytically active for the two epoxide substrates which were tested, although the reactivity was inferior to the structurally equivalent molecular analog of the catalyst. Future studies will focus on the variation of solid supports, notably including mesoporous oxides of varying pore sizes and morphologies to allow for cleaner diffusion of the substrates and products to and from the catalytic sites.

Acknowledgements

The authors would like to acknowledge funding from the French Ministry of Research (Project ANR-2010JCJC 7111 [(Sup)$_3$Base]). Sandrine Denis-Quanquin, Christine Lucas and Philippe Arquillière are also greatly thanked for their help in respectively solid-state NMR and TEM experiments.

Notes and references

1 J. G. Verkade, *Acc. Chem. Res.*, 1993, **26**, 483–489.
2 J. G. Verkade, *Coord. Chem. Rev.*, 1994, **137**, 233–298.
3 J. G. Verkade, *Top. Curr. Chem.*, 2002, **233**, 1–44.
4 J. G. Verkade and P. B. Kisanga, *Tetrahedron*, 2003, **59**, 7819–7858.
5 V. R. Chintareddy, K. Wadhwa and J. G. Verkade, *J. Org. Chem.*, 2009, **74**, 8118–8132.
6 K. Wadhwa, V. R. Chintareddy and J. G. Verkade, *J. Org. Chem.*, 2009, **74**, 6681–6690.
7 K. Wadhwa and J. G. Verkade, *J. Org. Chem.*, 2009, **74**, 5683–5686.
8 S. Urgaonkar and J. G. Verkade, *Org. Lett.*, 2005, **7**, 3319–3322.
9 P. Kisanga, X. Fei and J. Verkade, *Synth. Commun.*, 2002, **32**, 1135–1144.
10 L. Xiaodong and J. G. Verkade, *J. Org. Chem.*, 1999, **64**, 4840–4843.
11 B. M. Fetterly, N. K. Jana and J. G. Verkade, *Tetrahedron*, 2006, **62**, 440–456.
12 P. Dimitrov-Raytchev, J.-P. Dutasta and A. Martinez, *ChemCatChem.*, 2012, **4**, 2045–2049.
13 B. Chatelet, L. Joucla, J.-P. Dutasta, A. Martinez, K. C. Szeto and V. Dufaud, *J. Am. Chem. Soc.*, 2013, **135**, 5348–5351.
14 P. McMorn and G. J. Hutchings, *Chem. Soc. Rev.*, 1972, **33**, 108–122.
15 M. Heitbaum, F. Glorius and I. Escher, *Angew. Chem., Int. Ed.*, 2006, **45**, 4732–4762.
16 C. E. Song and S.-G. Lee, *Chem. Rev.*, 2002, **102**, 3495–3524.
17 A. P. Wight and M. E. Davis, *Chem. Rev.*, 2002, **102**, 3589–3614.
18 D. E. De Vos, M. Dams, B. F. Sels and P. A. Jacobs, *Chem. Rev.*, 2002, **102**, 3615–3640.
19 (*a*) H. C. Kolb, M. G. Finn and K. B. Sharpless, *Angew. Chem., Int. Ed.*, 2001, **40**, 2004–2021; (*b*) V. V. Rostovtsev, L. G. Green, V. V. Fokin and K. B. Sharpless, *Angew. Chem., Int. Ed.*, 2002, **41**, 2596.
20 V. Matsura, Y. Guari, J. Larionova, C. Guerin, A. Caneschi, C. Sangregorio, E. Lancelle-Beltran, A. Mehdi and R. J. P. Corriu, *J. Mater. Chem.*, 2004, **14**, 3026–3033.
21 Z. Guo, A. Lei, Y. Zhang, Q. Xu, X. Xue, F. Zhanga and X. Liang, *Chem. Commun.*, 2007, 2491–2493.
22 K. M. DiVittorio, F. T. Hofmann, J. R. Johnson, L. Abu-Esba and B. D. Smith, *Bioorg. Med. Chem.*, 2009, **17**, 141–148.
23 V. S. P. Lingam, R. Vinodkumar, K. Mukkanti, A. Thomas and B. Gopalan, *Tetrahedron Lett.*, 2008, **49**, 4260–4264.
24 T. Fukuyama, C.-K. Jow and M. Cheung, *Tetrahedron Lett.*, 1995, **36**, 6373–6374.
25 C. Lensink, S. K. Xi, L. M. Daniels and J. G. Verkade, *J. Am. Chem. Soc.*, 1989, **111**, 3478.
26 (*a*) C. T. Kresge, M. E. Leonowicz, W. J. Roth, J. C. Vartuli and J. S. Beck, *Nature*, 1992, **359**, 710–712; (*b*) J. S. Beck, J. C. Vartuli, W. J. Roth, M. E. Leonowicz, C. T. Kresge, K. D. Schmitt, C. T.-W Chu, D. H. Olson, E. W. Sheppard, S. B. McCullen, J. B. Higgins and J. L. Schlenker, *J. Am.*

Chem. Soc., 1992, **114**, 10834; (*c*) D. Zhao, J. Feng, Q. Huo, N. Melosh, G. H. Fredrickson, B. F. Chmelka and G. D. Stucky, *Science*, 1998, **279**, 548.

27 J. Nakazawa and T. D. Stack, *J. Am. Chem. Soc.*, 2008, **130**, 14360–14361.

28 (*a*) *Chemical Fixation of Carbon Dioxide: Methods for Recycling CO_2 into Useful Products*, ed. M. Halmann, CRC Press, Boca Raton, 1993; (*b*) *Carbon Dioxide as Chemical Feedstock*, ed. M. Aresta, Wiley-VCH, Weinheim, 2010; (*c*) T. Sakakura, J. C. Choi and H. Yasuda, *Chem. Rev.*, 2007, **107**, 2365–2387; (*d*) M. North, R. Pasquale and C. Young, *Green Chem.*, 2010, **12**, 1514–1539; (*e*) P. Pescarmona and M. Taherimehr, *Catal. Sci. Technol.*, 2012, **2**, 2169–2187.

29 (*a*) A. A. G. Shaikh and S. Sivaram, *Chem. Rev.*, 1996, **96**, 951; (*b*) B. Schäffner, F. Schäffner, S. P. Verevkin and A. Börner, *Chem. Rev.*, 2010, **110**, 4554; (*c*) D. J. Darensbourg, *Chem. Rev.*, 2007, **107**, 2388; (*d*) J. H. Clements, *Ind. Eng. Chem. Res.*, 2003, **42**, 663.

30 (*a*) W. J. Peppel, *Ind. Eng. Chem.*, 1958, **50**, 767; (*b*) S. Fukuoka, M. Kawamura, K. Komiya, M. Tojo, H. Hachiya, K. Hasegawa, M. Aminaka, H. Okamoto, S. Fukawa and S. Konno, *Green Chem.*, 2003, **5**, 497; (*c*) C. J. Harmsen, E. van der Heide and C. L. Vrouwenvelder, Process for the preparation of alkanediol, WO2004089866 (A1) 2004; (*d*) W. E. Evans, M. L. Hess, M. Matusz and E. M. G. van Kruchten, Process for the preparation of an alkylene carbonate and an alkylene glycol, WO2009140318 (A1), 2009; (*e*) T. Takahashi, T. Watahiki, S. Kitazume, H. Yasuda and T. Sakakura, *Chem. Comm.*, 2006, 1664–1666; (*f*) Y. Du, F. Cai, D. L. Kong and L. N. He, *Green Chem.*, 2005, **7**, 518–523; (*g*) J.-Q. Wang, D. L. Kong, J.-Y. Chen, F. Cai and L. N. He, *J. Mol. Catal. A: Chem.*, 2006, **249**, 143–148.

31 (*a*) A. Decortes, A. M. Castilla and A. W. Kleij, *Angew. Chem., Int. Ed.*, 2010, **49**, 9822; (*b*) T. Sakai, Y. Tsutsumi and T. Ema, *Green Chem.*, 2008, **10**, 337; (*c*) M. A. Fuchs, T. A. Zevaco, E. Ember, O. Walter, I. Held, E. Dinjus and M. Döring, *Dalton Trans.*, 2013, **42**, 5322–5329.

32 S. Udayakumar, M.-K. Lee, H.-L. Shim and D.-W. Park, *Appl. Catal., A*, 2009, **365**, 88–95.